Chapter 5

Extraction of Features from the Segmented Objects

The extraction of effective features from the segmented images of parasitic eggs is crucial for accurate identification. After segmenting the parasite eggs from microscopic images, the next step is to extract features that accurately represent the underlying structures and are robust to variations in imaging conditions and species of parasite eggs. These features are key to developing classification models that can accurately distinguish between different types of parasitic eggs and other objects.

Robustness is a key factor in feature extraction, ensuring that the features remain consistent and informative across diverse classes and datasets. Features must endure variations in image quality, lighting conditions, and specimen preparation techniques. Texture descriptors, such as Haralick features or local binary patterns, are commonly used to capture spatial patterns and variations in pixel intensities, providing valuable information about the surface characteristics of parasitic eggs. Shape-based features, which focus on geometric properties like circularity and compactness, also enhance the robustness of the feature sets.

Efficiency in feature extraction is crucial, especially with large-scale image datasets. The computational demands require methods that are both accurate and computationally efficient. Dimensionality reduction methods may speed up computation by transforming the feature space into a lower-dimensional subspace while preserving maximum variance. This not only accelerates classification algorithms but also helps address the challenges associated with high-dimensional data analysis.

After thoroughly exploring different types of features, six different types of feature sets are extracted from the segmented objects. These include various image moments such as Hu's moments, Legendre moments, Chebyshev moments, and Krawtchouk moments. These mathematical descriptors provide a deep understanding of the spatial distribution and shape characteristics within the images. This work also incorporates texture features and shape-based features, enabling a more detailed investigation of the objects' surface patterns and geometric structures. Additionally, a grayscale pixel intensity-based feature set is included, offering insights into the objects' shading differences and contrasts. Details of these feature sets are discussed in the following sections.

5.1 Image Moment-Based Features

Image moments are mathematical features used in image processing to quantify and characterize various properties of an image. These moments provide a compact representation of the spatial distribution of pixel intensities, offering valuable insights into the shape, structure, and other essential features of an image. The general formula for computing moments of an image function f(x,y) is given by:

$$M_{pq} = \Sigma_x \Sigma_y x^p y^q f(x, y) \tag{5.1}$$

where M_{pq} represents the p^{th} order and q^{th} order moments of the image. Two commonly used moments include the first-order moment, or mean, and the central moment. First-order moment, or Mean (M_{pq}), which is computed as the summation of pixel intensities, weighted by their spatial positions, as mentioned in equation 5.2. Normalized first-order moments, μ_{pq}, provide information about the centre of mass of the image. Central moments, (η_{pq}), are normalized versions of raw moments computed as shown in Equation 5.3, providing translational invariance. They are particularly valuable for characterizing the shape of objects in an image.

$$\mu_{pq} = \frac{M_{pq}}{M_{00}} \tag{5.2}$$

$$eta_{pq} = \frac{M_{pq}}{M_{00}^{\frac{p+q}{2}+1}} \tag{5.3}$$

Higher-order moments, such as Hu moments [117], enhance robustness against scale and rotation, making them valuable in pattern recognition and object analysis. In general, image moments play an important role in feature extraction, facilitating the development of effective algorithms for tasks like object recognition, shape analysis, and machine learning across various computer vision applications. After a thorough study of various types of image moments, four distinct sets of moments are computed to prepare four types of feature vectors. These image moments are outlined below:

5.1.1 Hu Moments

Hu moments, introduced by Ming-Kuei Hu [117], are a set of seven moments widely used in image processing for shape analysis and pattern recognition. These moments are invariant to translation, rotation, and scale, making them robust features for various computer vision applications. The orthogonality of Hu moments simplifies computations and enhances stability [47]. They offer a unique representation for each object and provide a compact feature set, which is advantageous in applications with limited computational resources. The Hu moments are derived from the central moments of an image. They offer a concise representation of an object's shape, enabling efficient and effective recognition. The equations for calculating Hu moments are as follows:

$$
\begin{aligned}
\mathrm{Hu}_1 &= \eta_{20} + \eta_{02} \\
\mathrm{Hu}_2 &= (\eta_{20} - \eta_{02})^2 + 4\eta_{11}^2 \\
\mathrm{Hu}_3 &= (\eta_{30} - 3\eta_{12})^2 + (3\eta_{21} - \eta_{03})^2 \\
\mathrm{Hu}_4 &= (\eta_{30} + \eta_{12})^2 + (\eta_{21} + \eta_{03})^2 \\
\mathrm{Hu}_5 &= (\eta_{30} - 3\eta_{12})(\eta_{30} + \eta_{12})[(\eta_{30} + \eta_{12})^2 - 3(\eta_{21} + \eta_{03})^2] \\
\mathrm{Hu}_6 &= (\eta_{20} - \eta_{02})[(\eta_{30} + \eta_{12})^2 - (\eta_{21} + \eta_{03})^2] + 4\eta_{11}(\eta_{30} + \eta_{12})(\eta_{21} + \eta_{03}) \\
\mathrm{Hu}_7 &= (3\eta_{21} - \eta_{03})(\eta_{30} + \eta_{12})[(\eta_{30} + \eta_{12})^2 - 3(\eta_{21} + \eta_{03})^2] - (\eta_{30} - 3\eta_{12})(\eta_{21} + \eta_{03}) \\
&\quad [3(\eta_{30} + \eta_{12})^2 - (\eta_{21} + \eta_{03})^2]
\end{aligned}
\tag{5.4}
$$

Here, η_{20} and η_{02} capture information about the shape's elongation or roundness. They are invariant to scale and rotation. η_{11} is a measure of the correlation between x and y coordinates. It provides information about the orientation of the shape and is invariant to rotation. η_{30} and η_{03} capture information about the shape's skewness and are invariant to scale, rotation, and reflection. η_{12} and

η_{21} capture information about the shape's tilt and are invariant to scale, rotation, and reflection. Hu Moments offer a simplified and reliable representation of an object's shape in an image, making them useful for computer vision applications such as image matching and object recognition where shape information is required.

In general, Hu moments for an image are computed from the entire image. However, in many cases, it is seen that the parasite egg is not centred in the segmented image. Extracting features from the whole image may include redundant information, which can lead to misclassification. To extract features solely from the parasite egg and avoid background, an approach utilizing the binary-segmented images as a mask is applied. The steps involved in the process are given below:

Step 1: Determine the boundary pixel coordinates of the object in the segmented image.

Step 2: Match the pixel coordinates with the corresponding grayscale image.

Step 3: Extract the pixel values that are inside the boundary of the object in grayscale

Step 4: Use only these pixels to extract the feature.

5.1.2 Legendre Moments

Legendre moments are a set of mathematical descriptors used for representing the shape and structure of functions or signals. They are introduced by Michael Reed Teague [118], using the Legendre polynomials, which are a family of orthogonal polynomials defined on the interval [-1, 1] [118–120]. These orthogonal moments are robust in the presence of noise and invariance to rotation and scale transformations, allowing them to be used in a variety of computer vision and image processing applications. Legendre moments of order (m+n) are defined as equation 5.5[119, 120]:

$$\lambda_{mn} = \frac{(2m+1)(2n+1)}{4} \int_{-1}^{1} \int_{-1}^{1} P_m(x) P_n(y) f(x,y) dx dy; \qquad [m,n] \in [-1,1] \tag{5.5}$$

The *pth* order Legendre polynomials can be defined as in Equation 5.6 [47,119,121]:

$$P_p(x) = \frac{(-1)^p}{2^2 p!} (\frac{d}{dx})^p [(1-x^2)^p] \tag{5.6}$$

For a discrete image of size $M \times N$ pixels and intensity function $f(i,j)$ where $i \leq M$ and $j \leq N$, the Legendre moments (λ_{mn}) can be approximated as below [47, 120]:

$$\lambda_{mn} = \frac{(2m+1)(2n+1)}{(M-1)(N-1)} \sum_{i=1}^{M} \sum_{i=1}^{N} P_m(x) P_n(x) f(x_i, y_j) \tag{5.7}$$

where $x_i = \frac{2i-M-1}{M-1}$ and $y_j = \frac{2j-N-1}{N-1}$.

Instead of using this approximation, an efficient way, proposed by Simon X. Liao and Miroslaw Pawlak is used as shown in Equation 5.8 [120, 122].

$$\tilde{\lambda_{mn}} = \frac{(2m+1)(2n+1)}{(M-1)(N-1)} \sum_{i=1}^{M} \sum_{i=1}^{N} h_{mn}(x_i, y_j) f(x_i, y_j) \tag{5.8}$$

where,

$$h_{mn}(x_i, y_j) = \int_{x_i - \Delta x/2}^{x_i + \Delta x/2} \int_{y_j - \Delta y/2}^{y_j + \Delta y/2} P_m(x) P_n(y) dx dy; \tag{5.9}$$

where, $\Delta x = \frac{2}{M-1}$ and $\Delta y = \frac{2}{N-1}$

5.1.3 Chebyshev Moments

The Chebyshev moments are derived from the discrete Chebyshev polynomials and play a significant role in image processing and pattern recognition. One of the major advantages of the Chebbyshev moment is its ability to efficiently capture image characteristics with fewer coefficients, resulting in a compact representation. Chebyshev moments are particularly useful in scenarios where computational efficiency is crucial. Moreover, these moments possess desirable orthogonality properties, making them robust against noise and ensuring reliable feature extraction.

Given an image of size NXN pixels and an intensity function $f(x,y)$ where x and y are the pixel coordinates, the Chebyshev moments C_pq of order $(p+q)$ can be computed as follows [119, 123]:

$$C_{pq} = \frac{1}{\rho(p,N)\rho(q,N)} \sum_{x=0}^{N-1} \sum_{y=0}^{N-1} t_p(x) t_q(y) f(x,y) \tag{5.10}$$

where $\rho(p, N)$ is calculated as equation 5.11

$$\rho(p,N) = \frac{N(1-\frac{1}{N^2})(1-\frac{2^2}{N^2})(1-\frac{3^2}{N^2})...(1-\frac{p^2}{N^2})}{2p+1} \tag{5.11}$$

The scaled Chebyshev polynomials $t_p(x)$ are calculated using the recurrence relation as Equation 5.12 [124]:

$$t_p(x) = \frac{(2p-1)t_1(x)t_{p-1}(x) - (p-1)\{1-\frac{(p-1)^2}{N^2}\}t_{p-2}(x)}{p}, \qquad p > 1 \tag{5.12}$$

where $t_0(x) = 1$ and $t_1(x) = \frac{2x+1-N}{N}$. As p rises, the value of $\rho(p, N)$ approaches zero. Thus, when either p or q is large, Equation 5.10 yields very large values [119]. The issue can be solved using the orthonormal form of the moments proposed in [124]. The orthonormal Chebyshev polynomials are calculated by the recurrence relation as given below [119]:

$$\tilde{t}_p(x) = \alpha(2x+1-N)\tilde{t}_{p-1}(x) + \beta\tilde{t}_{p-2}(x); \qquad p = 0,1,...,N-2; x = 0,1,...,N-1 \tag{5.13}$$

where,

$$\alpha = \frac{\sqrt{4p^2-1}}{p\sqrt{N^2-p^2}}, \qquad \beta = -\frac{(p-1)\sqrt{2p+1}\sqrt{N^2-(p-1)^2}}{p\sqrt{2p-3}\sqrt{N^2-p^2}}$$

The initial conditions for Equation 5.13 are as follows:

$$\tilde{t}_0(x) = N^{-1/2} \tag{5.14}$$

$$\tilde{t}_1(x) = \frac{\sqrt{3}(2x+1-N}{\sqrt{N(N^2-1)}} \tag{5.15}$$

To reduce the impact of any numerical errors, the polynomials provided in Equation 5.13 can be re-normalized as follows:

$$\tilde{t}_p(x) = \frac{\tilde{t}_p(x)}{\sqrt{\sum_{x=0}^{N-1}(\tilde{t}_p(x))^2}} \tag{5.16}$$

The orthonormal Chebyshev polynomials are calculated using the recurrence relation given below [119]

$$C_{pq} = \sum_{x=0}^{N-1} \sum_{y=0}^{N-1} \tilde{t}_p(x)\tilde{t}_q(y)f(x,y); \qquad p,q = 0,1,2,....,N-1 \tag{5.17}$$

For an image of size $M \times N$, the above equation can be represented as follows:

$$C_{pq} = \sum_{x=0}^{M-1} \sum_{y=0}^{N-1} \tilde{t}_p(x)\tilde{t}_q(y)f(x,y); \qquad p = 0,1,2,....,M-1; q = 0,1,2,....,n-1 \tag{5.18}$$

In this study, the normalized orthonormal Chebyshev form is used. In the discrete domain of image coordinate space, the basis functions of Chebyshev moments are orthogonal, which means no discrete approximation is needed for their implementation. This also removes the need for coordinate space normalisation. The Chebyshev moments are computed directly using Equations 5.17 and 5.18.

5.1.4 Krawtchouk moments

The Krawtchuk moments are mathematical features employed in image processing and pattern recognition to analyze and represent spatial patterns within images. These moments are derived from the Krawtchuk polynomials, originally introduced by Pew-Thian Yap [125, 126]. These polynomials are orthogonal and defined on a finite domain, closely associated with the binomial distribution [126]. The $(p+q)$-th order Krawtchouk moments of an image with an intensity function $f(x,y)$ can be calculated as below: [126]:

$$Q_{pq} = \sum_{x=0}^{N-1} \sum_{y=0}^{N-1} \bar{K}_p(x;t_1,N-1)\bar{K}_q(y;t_2,N-1)f(x,y) \tag{5.19}$$

where $\bar{K}_p(x;t_1,N-1)$ is the pth order weighted Krawtchouk polynomial defined as

$$\bar{K}_p(x;t_1,N-1) = K_p(x;t_1,N-1)\sqrt{\frac{\omega(x;t,N-1)}{\rho(p;t,N-1)}} \tag{5.20}$$

Here $K_p(x; t_1, N-1)$ is the pth discrete Krawtchouk moments, which are defined as follows:

$$K_p(x; t_1, N-1) = \sum_{k=0}^{p} a_k, p, tX^k = {}_2F_1(-p, -x, (N-1); \frac{1}{t}) \\ x, p = 0, 1, 2, N-1; \quad N-1 > 0; \quad t \in (0, 1) \tag{5.21}$$

Where, ${}_2F_1$ is known as a hyper-geometric function, which can be calculated as:

$${}_2F_1(a, b; c; z) = \sum_{k=0}^{\infty} \frac{(a)_k (b)_k z^k}{(c)_k k!} \tag{5.22}$$

and a_k is the Pochhammer symbol, defined as:

$$a_k = a(a+1)...(a+k-1) = \frac{\Gamma(a+k)}{\Gamma(a)} \tag{5.23}$$

The set of Krawtchouk polynomials defined by Equation 5.21 forms an entire set of discrete basis functions with a weight function as given below:

$$\omega(x; t, N-1) = \binom{N-1}{x} t^x (1-t)^{N-1-x} \tag{5.24}$$

For a $M \times N$-sized image, Equation 5.19 can be rewritten as follows:

$$\sum_{x=0}^{M-1} \sum_{y=0}^{N-1} \bar{K}_p(x; t_1, M-1) \bar{K}_q(t; t_2, N-1) f(x, y) \tag{5.25}$$

Recurrence relations are useful in computing Krawtchouk polynomials to prevent overflow when dealing with mathematical functions such as Equation 5.22 and gamma functions. The recursive relation for the weighted Krawtchouk polynomials is provided as follows [126]:

$$\bar{K}_{p+1}(x; t, N-1) = \frac{A((N-1)t - 2_p t + p - x)}{t(N-1-p)} \bar{K}_p(x; t, N-1) - \frac{B_p(1-t)}{t(N-1-p)} \bar{K}_{p-1}(x; t, N-1), \\ p = 1, 2, 3, ..., N-2 \tag{5.26}$$

where, $A = \sqrt{\frac{t(N-1-p)}{(1-t)(p+1)}}$, and $B = \sqrt{\frac{t^2(N-1-p)(N-p)}{(1-t)^2(p+1)p}}$, with $\bar{K}_0(x;t,N-1) = \sqrt{\omega(x;t,N-1)}$ and $\bar{K}_1(x;t,N-1) = (1-\frac{x}{t(N-1)})(\sqrt{\frac{t(N-1)}{1-t}})\sqrt{\omega(x;t,N-1)}$

Similarly, the weight function as provided in Equation 5.24 can also be computed using the following recursive relation:

$$\omega(x+1;t,N-1) = (\frac{N-1-x}{x+1})\frac{t}{1-t}\omega(x;t,t,N-1) \tag{5.27}$$

where, $\omega(0;t,N-1) = (1-t)^{N-1}$

Using the symmetry property for the specific scenario $t_1 = t_2 = 0.5$ can greatly reduce the computation time of the Krawtchouk moments. The weighted Krawtchouk polynomial's symmetry relation is provided by the equation [126].

$$\bar{K}_p(x;t_1,N-1) = (-1)^p\bar{K}_p(N-1-x;t,N-1) \tag{5.28}$$

Krawtchouk moments have base functions that are orthogonal in the discrete domain of the image coordinate space, much like Chebyshev moments. Coordinate-space normalization and discrete approximation are therefore not necessary for the execution of these moments.

5.2 Texture and Shape-based Features

Image texture features refer to the patterns and variations in intensity within an image, providing crucial information about the spatial arrangement of pixel values. Texture features capture properties like smoothness, coarseness, and regularity, enabling the characterization of various patterns and objects within an image. In the field of parasite egg identification in microscopic images, texture features play a crucial role. Microscopic images of parasite eggs often exhibit distinct textural patterns that are indicative of the specific parasite species. Analyzing the texture features helps in differentiating between various egg types based on their surface characteristics, allowing for more accurate and efficient identification.

Haralick features, also known as GLCM (Gray-Level Co-occurrence Matrix) features, are a well-known set of features widely used in image analysis.

Developed by Robert M. Haralick et al. [127] in the 1970s, these features are significant for their ability to quantify complex texture patterns within images. In this work, Haralick features and the GLCM framework are used to analyze the internal patterns of various parasite eggs and non-egg objects in microscopic images of fecal samples.

5.2.1 Grey-Level Co-occurrence Matrix

Gray-Level Co-occurrence Matrix or Gray-level Spatial Dependence Matrix is a statistical method for examining texture based on the spatial relationship of pixels in a gray-scale image [128]. The GLCM works by examining how frequently certain pairs of pixels appear in a picture, considering their specific values and their relative positions. Based on this information, it constructs a matrix from which statistical metrics are subsequently extracted to quantify and describe the textural properties of the image.

The GLCM of a grayscale image I, which is normalized in n-dimensional Euclidean space Z^n, can be defined as a square matrix G_d of size N, where N represents the total number of gray levels [129]. The value at position $(i,j)^{th}$ in the matrix G_d indicates the frequency of occurrences of a pixel X, having intensity value i, located at a specific distance k from another pixel Y with an intensity value j in a given direction d. Where k is a positive integer value and d is defined as: $d = (d_1, d_2, d_3, ..., d_n)$; $d_i \in \{0, k, -k\}, \forall i = 1, 2, 3, ..., n$.

Let's consider a grayscale image in Z^3 space with intensity values 0, 1, 2, and 3. The image can be represented as a three-dimensional matrix of size $3 \times 3 \times 3$, where each of the three slices can be illustrated as follows [129]:

$$\begin{bmatrix} 0 & 0 & 1 \\ 0 & 1 & 2 \\ 0 & 2 & 3 \end{bmatrix} \quad \begin{bmatrix} 1 & 2 & 3 \\ 0 & 2 & 3 \\ 0 & 1 & 2 \end{bmatrix} \quad \begin{bmatrix} 1 & 3 & 0 \\ 0 & 3 & 1 \\ 3 & 2 & 1 \end{bmatrix}$$

The 3-D co-occurrence matrix G_d for the given image along the direction $d = (1, 0, 0)$ can be represented as a 4×4 matrix, as illustrated below:

$$G_d = \begin{bmatrix} 1 & 3 & 1 & 1 \\ 0 & 0 & 3 & 1 \\ 0 & 1 & 0 & 3 \\ 1 & 1 & 1 & 0 \end{bmatrix}$$

The Haralick texture features are derived from the normalized GLCM, representing various characteristics of the gray-level distribution within the image [130]. Normalized GLCM can be defined as follows [129]:

$$GN_d = \frac{1}{N} G_d(i,j) \tag{5.29}$$

Where, N represents the total number of co-occurrence pairs in G_d and is defined as follows:

$$N = \sum_{i,j} G_d(i,j) \tag{5.30}$$

The value at position (i,j) in GN_d represents the joint probability of pixels with intensity i and j appearing together at a distance k in a specified direction d.

5.2.2 Haralick Texture Features

Haralick et al. [127] described fourteen types of texture features that can be extracted using normalized gray-level co-occurrence matrices. These features and the corresponding equations used to compute them are listed below:

1. **Angular second moment:**

$$f_1 = \sum_i \sum_j p(i,j)^2 \tag{5.31}$$

2. **Contrast:**

$$f_3 = \sum_{i=1}^{N_g} \sum_{j=1}^{N_g} (i-j)^2 p(i,j) \tag{5.32}$$

3. **Correlation:**

$$f_3 = \frac{\sum_{i=1}^{N_g} \sum_{j=1}^{N_g} (ij) p(i,j) - \mu_x \mu_y}{\sigma_x \sigma_y} \tag{5.33}$$

where μ_x, μ_y are means and σ_x, σ_y are the standard deviations of p_x and p_y.

4. **Sum of squares: Variance:**

$$f_4 = \sum_{i=1}^{N_g} \sum_{j=1}^{N_g} (i - \mu)^2 p(i, j) \tag{5.34}$$

5. **Inverse Difference Moment:**

$$f_5 = \sum_{i=1}^{N_g} \sum_{j=1}^{N_g} \frac{1}{1 + (i - j)^2} p(i, j) \tag{5.35}$$

6. **Sum Average:**

$$f_6 = \sum_{i=2}^{2N_g} i p_{x+y}(i) \tag{5.36}$$

7. **Sum Variance:**

$$f_7 = \sum_{i=2}^{2N_g} (i - f_8)^2 p_{x+y}(i) \tag{5.37}$$

8. **Entropy:**

$$f_9 = -\sum_{i=1}^{N_g} \sum_{j=1}^{N_g} p(i, j) \log(p(i, j)) \tag{5.38}$$

9. **Sum Entropy:**

$$f_9 = -\sum_{i=2}^{2N_g} p_{x+y}(i) \log(p_{x+y}(i)) \tag{5.39}$$

10. **Difference Variance:**

$$f_{10} = \sum_{k=0}^{N-1} (k - \mu_{x-y})^2 p_{x-y}(k) \tag{5.40}$$

11. **Difference Entropy:**

$$f_{11} = -\sum_{i=0}^{N_g - 1} p_{x-y}(i) \log(p_{x-y}(i)) \tag{5.41}$$

12. **Information Measure of Correlation-1:**

$$f_{12} = \frac{HXY - HXY1}{\max(HX, HY)} \tag{5.42}$$

13. **Information Measure of Correlation-2:**

$$f_{13} = \sqrt{1 - \exp[-2(HXY2 - HXY)]} \tag{5.43}$$

14. **Maximal Correlation Coefficient:**

$$f_{14} = (\text{Second largest eigenvalue of } Q)^2 \tag{5.44}$$

Where $Q(i,j) = \sum_k \frac{p(i,k)p(j,k)}{p_x(i)p_y(k)}$.

The above equations use various terms and notations, such as $p(i)$, $p(y)$, HX, HY, etc., which are defined as follows:

- $p(i,j) = \frac{P(i,j)}{R}$ is the co-occurrence probability matrix.
- $p_x(i) = \sum_{j=1}^{N_g} p(i,j)$ is the i^{th} entry in the marginal-probability matrix obtained by summing the rows of $p(i,j)$.
- $p_y(j) = \sum_{i=1}^{N_g} p(i,j)$ is the j^{th} entry in the marginal-probability matrix obtained by summing the columns of $p(i,j)$.
- $p_{x+y}(k) = \sum_{i=1}^{N_g} \sum_{j=1}^{N_g} p(i,j)$, where $k = 2, 3, ..., 2N_g$.
- $p_{x-y}(k) = \sum_{i=1}^{N_g} \sum_{j=1}^{N_g} p(i,j)$, where $k = 0, 1, ..., N_g - 1$.
- $HX = -\sum_i p_x(i) \log(p_x(i))$ is entropy of p_x.
- $HY = -\sum_j p_y(j) \log(p_y(j))$ is entropy of p_y.
- $HXY = -\sum_i \sum_j p(i,j) \log(p(i,j))$
- $HXY1 = -\sum_i \sum_j p(i,j) \log(p_x(i)p_y(j))$.
- $HXY2 = -\sum_i \sum_j p_x(i)p_y(j) \log(p_x(i)p_y(j))$.

5.2.3 Shape-based Descriptors

Along with the texture features, four simple shape-based features, viz., area, perimeter, circularity, and accept ratio are also incorporated to make the feature vector more robust and effective. These shape features are calculated as follows:

- **Area:** It represents the total number of the object's pixels that belong to the specified object. The area of a segmented object of size $M \times N$ is calculated using the binary-segmented mask of the object as follows:

$$Area = \sum_{i=1}^{M} \sum_{j=1}^{N} \mathbb{I}(x_{ij} = 1) \tag{5.45}$$

where, $\mathbb{I}$ is the indicator function that is used to include the pixels x_{ij} that are equal to 1 (white pixel) and 0 (dark pixel) otherwise.

- **Perimeter:** We approximated the perimeter by counting the number of boundary pixels of the segmented objects as follows [131]:

$$Perimeter = \sum_{i=1}^{N-1} |x_i - x_{i+1}| \tag{5.46}$$

where, N is the total number of boundary pixels.

- **Circularity:** Circularity is a shape descriptor that indicates how close an object's shape is to that of a perfect circle. The following equation is used to calculate the circularity of a segmented object [132]:

$$Circularity = \frac{4\pi \times \text{Area}}{\text{Perimeter}^2} \tag{5.47}$$

- **Accept Ratio:** The aspect ratio is a measure of how elongated or stretched an object is. The aspect ratio of an object in a binary image can be calculated by determining the ratio of its major axis length to its minor axis length as follows:

$$AspectRatio = \frac{\text{Major Axis Length}}{\text{Minor Axis Length}} \tag{5.48}$$

5.2.4 Pixel Intensity-based Feature

In image analysis, pixel intensity-based features offer valuable information about the grayscale and colour distribution of an image. Features like mean and median pixel intensity, standard deviation, and minimum and maximum intensity, among others, are commonly extracted to characterize the overall intensity properties. However, focusing solely on these features from entire segmented images of parasite eggs may overlook important local patterns such as edge thickness and internal textures of objects like parasite eggs. To obtain more detailed information, the segmented grayscale images are divided multiple into uniformly sized blocks, and

features are extracted from each block, as illustrated in Figure 5-1. The final feature vector is then constructed by combining the values from all the blocks.

To evaluate the effectiveness of the feature set, several experiments using different block sizes: 20×20, 30×30, 40×40, and 60×60 pixels, are conducted. Each block size generates a distinct feature set, which is evaluated individually during the classification stage to determine the optimal block size for image division. This block-wise, pixel intensity-based feature set provides a detailed characterization of the segmented object's grayscale properties and allows to capture local variations within the object. In this study, the following five intensity-based features are extracted:

- **Mean Intensity:** The mean intensity represents the average pixel value within the segmented object and is calculated as:

$$Mean \quad Intensity = \frac{\sum_{i=1}^{N} I_i}{N} \tag{5.49}$$

- **Maximum Intensity:** The maximum intensity represents the highest pixel value within the segmented object and is calculated as:

$$Maximum \quad Intensity = \max_{i=1}^{N} I_i \tag{5.50}$$

- **Minimum Intensity:** Conversely, the minimum intensity represents the lowest pixel value within the segmented object and is calculated as:

$$Minimum \quad Intensity = \min_{i=1}^{N} I_i \tag{5.51}$$

- **Variance**: Variance measures the spread or dispersion of pixel intensities within the segmented object and is calculated as:

$$Variance = \frac{\sum_{i=1}^{N} (I_i - \text{Mean Intensity})^2}{N} \tag{5.52}$$

- **Standard deviation:** Standard deviation quantifies the degree of deviation of individual pixel intensities from the mean intensity and is calculated as:

$$Standard \quad Deviation = \sqrt{\frac{\sum_{i=1}^{N} (I_i - \text{Mean Intensity})^2}{N}} \tag{5.53}$$

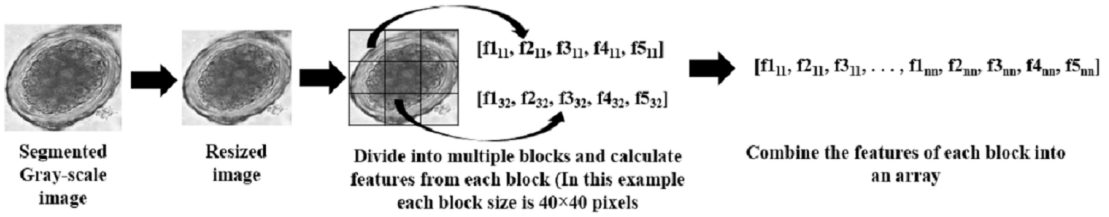

Figure 5-1: Process of Extracting Pixel Intensity-based Features. Here, f1, f2, f3, f4, and f5 represent mean, maximum, minimum pixel intensity, variance, and standard deviation, respectively.

5.3 Conclusion

In this chapter, the detailed process of feature extraction from segmented images of parasite eggs and non-egg objects is discussed. Different types of feature sets are carefully selected and extracted with the aim of effectively classifying parasite eggs and distinguishing them from non-egg objects. The key contributions of the chapter include:

- Selection and extraction of feature sets: Based on the extensive literature review, six feature sets are selected and extracted from the segmented objects.
- Utilization of various image moments-based features: Four different kinds of image moments, namely: Hu's invariant moments, Legendre moments, Chebyshev moments, and Krawtchuk moments, are extracted from the segmented grayscale object images.
- Extraction of texture-based features: From the Gray Level Co-occurrence Matrix (GLCM), of the images, fourteen texture features are extracted. These texture feature are then combined with a few shape-based features, including area, perimeter, circularity, and aspect ratio, for optimal classification results.
- Extraction of pixel intensity-based features: This chapter proposes a method for extracting basic pixel intensity values such as mean, maximum, minimum intensity, variance, and standard deviation from segmented objects to create an effective feature set for classification of parasite eggs.